Available online at www.sciencedirect.com
SCIENCE DIRECT®
Organic Geochemistry 35 (2004) 73–89
Organic Geochemistry
www.elsevier.com/locate/orggeochem

Trapping hydropyrolysates on silica and their subsequent thermal desorption to facilitate rapid fingerprinting by GC–MS

Will Meredith[a], Christopher A. Russell[a], Mick Cooper[a], Colin E. Snape[a,*], Gordon D. Love[b], Daniele Fabbri[c], Christopher H. Vane[d]

[a]*Nottingham Fuel & Energy Centre, School of Chemical, Environmental and Mining Engineering, University of Nottingham, University Park, Nottingham NG7 2RD, UK*
[b]*School of Civil Engineering and Geosciences, Drummond Building, University of Newcastle, Newcastle upon Tyne NE1 7RU, UK*
[c]*Laboratorio di Chimica Ambientale, Università di Bologna, via Marconi 2, 48100 Ravenna, Italy*
[d]*British Geological Society, Keyworth, Nottingham NG12 5GG, UK*

Received 7 January 2003; accepted 22 July 2003
(returned to author for revision 5 May 2003)

Abstract

Analytical hydropyrolysis performed under high hydrogen gas pressure (>10 MPa) has been demonstrated to possess the unique ability to release high yields of biomarker hydrocarbons covalently bound within the non-hydrocarbon macromolecular fraction of crude oils and source rocks. This study describes the development of the experimental procedure for trapping the product oils (hydropyrolysates) on silica to facilitate more convenient recovery than conventional collection and to allow analysis by thermal desorption-GC–MS without any prior work-up. Conventionally, the trap has consisted of a stainless steel coil, cooled with dry ice from which the products are recovered in organic solvents. Replacing this with a system in which the hydropyrolysates are adsorbed on a small mass of silica greatly reduces the turn-around time between tests, and aids the recovery and separation of the products. This method has been developed using an oil shale and an oil asphaltene fraction, with the silica trap producing very similar biomarker profiles to that from the conventional trap. The quantitative recovery of hydrocarbons from a light crude oil desorbed from silica under hydropyrolysis conditions demonstrates no significant loss of the high molecular weight *n*-alkanes (>*n*-C_{10}) for both trapping methods. The use of liquid nitrogen as the trap coolant results in significantly improved recovery of the lower molecular mass constituents. The silica trapping method allows for the hydropyrolysates to be characterised by thermal desorption-GC–MS, which has been investigated both on- and off-line. The oils undergo relatively little cracking during desorption, with similar *n*-alkane and biomarker profiles being obtained as with normal work-up and GC–MS analysis. Thus, in terms of fingerprinting geomacromolecules, "hypy-thermal desorption-GC–MS" appears to have the potential to be developed as an attractive alternative to traditional py-GC–MS.

1. Introduction

Fixed-bed hydropyrolysis of coals and oil shales at high hydrogen pressures (>10 Mpa), together with the use of a dispersed sulfided molybdenum catalyst has been demonstrated to give rise to high yields (>65 wt.%) of dichloromethane (DCM) soluble products,

* Corresponding author. Tel.: +44-115-9514166; fax: +44-115-9514115.
E-mail address: colin.snape@nottingham.ac.uk (C.E. Snape).

0146-6380/$ - see front matter © 2003 Elsevier Ltd. All rights reserved.
doi:10.1016/j.orggeochem.2003.07.002

with overall conversions greater than 85 wt.% of the total organic matter (Lafferty et al., 1993; Snape et al., 1994; Roberts et al., 1995). The use of a slow heating rate (5–10 °C min^{-1}) for the hydropyrolysis of organic matter-rich samples generates a high yield of hydrocarbon biomarkers such as hopanes and steranes, whilst minimising the alteration to their isomeric distributions, as demonstrated by the preservation in hydropyrolysates from source rock kerogens, lignite and recent sediments of hopanes with the biologically inherited, but thermodynamically unstable 17β(H),21β(H) configuration (Robinson et al., 1991; Love et al., 1995, 1996, 1997; Murray et al., 1998; Bishop et al., 1998). These characteristics allow for the bound biomarkers released by hydropyrolysis to offer potential solutions to tackling many problems in oil exploration where the conventional geochemical approach using the free (extractable) hydrocarbon biomarkers cannot be employed, such as for severely degraded oils where pristine biomarker profiles have been obtained from asphaltenes (Murray et al., 1999) and where hydrocarbon oil-based drilling mud contamination is encountered (Murray et al., 1998).

Hydropyrolysis has also been demonstrated to allow a greater precision in the determination of thermal maturity of source rocks and heavy oil fractions than is possible with traditional, free biomarker procedures (Murray et al., 1998). The technique is currently being used to elucidate the filling history of mixed reservoirs, with the asphaltenes most strongly bound to core samples believed to be representative of the first charge of oil encountered. This work will be the subject of a subsequent paper. Due to the minimal structural alteration, and net hydrogenation (bulk addition of H atoms) which occurs during hydropyrolysis, the products have similar bulk skeletal parameters, such as carbon aromaticity and long alkyl chain contents, to those of their parent kerogens (Maroto-Valer et al., 1997).

Although generally more rapid than the closed system pyrolysis methods which have been utilised for generating bound biomarker profiles from geomacromolecules in correlation studies (Rubinstein et al., 1979; Curiale et al., 1983; Cassani and Eglinton, 1986; Jones et al., 1987, 1988; Connan, 1993), hydropyrolysates have traditionally been recovered for subsequent fractionation and analysis in dichloromethane from a coiled trap cooled with dry ice. Whilst providing a satisfactory means of recovery, this procedure is relatively time consuming, requiring repeated solvent extraction of the trap, resulting in a long turn-around time between experiments. This study firstly describes the development of an alternative trapping method, in which the hydropyrolysates are adsorbed directly on to a small mass of silica, from which they can be desorbed with solvent or fractionated as required. The quantitative recovery of individual components generated during hydropyrolysis is described, although the high yields reported in previous studies suggest that the conventional trapping method is not subject to significant losses.

In addition to accelerating the recovery of the product, the silica trapping procedure also allows for the hydropyrolysates to be thermally desorbed from the silica for direct analysis by GC–MS, negating the need for solvent extraction or fractionation of the products. Although analytical pyrolysis methods for the structural characterisation of kerogens and asphaltenes, with the pyrolyser coupled directly to a gas chromatograph (py-GC) (e.g. Larter et al., 1979; Behar et al., 1984; Behar and Pelet, 1984, 1985) a mass spectrometer (py-MS) (e.g. Eglinton et al., 1991) or a py-GC–MS system (e.g. Gallegos, 1975; Philip and Gilbert, 1985; van Graas, 1986), are well-established (for a review of analytical pyrolysis, see Larter and Horsfield, 1993), due to the low yields and the cracking undergone, pyrolysates are, at best, only partially representative of the bulk kerogen structure (Love et al., 1995). This study describes the thermal desorption of the hydropyrolysate for a type I kerogen trapped on silica both on-line and off-line, with the resultant yields and biomarker profiles compared to those obtained from the traditional recovery and fractionation procedure.

2. Experimental

2.1. Samples

The samples used to assess the silica trapping procedure for recovering hydropyrolysates were the Göynük oil shale (GOS) and the asphaltene fraction isolated from a biodegraded crude oil (Soldado Field, Trinidad—marine carbonate source). The thermal desorption experiments have been performed on the hydropyrolysate of the GOS. This lacustrine oil shale of Tertiary age has been classified as a type I kerogen (Love et al., 1995, 1997, 1998). It was pre-extracted with DCM/methanol (93:7 v/v), washed with dilute HCl (2M) at 50 °C for 3 h and re-extracted with DCM/methanol (93:7 v/v), so any products generated would be predominantly released from the kerogen phase. The asphaltenes were isolated from the Trinidadian oil by four sequential dissolutions of the maltene fraction in an excess of *n*-heptane, with the insoluble asphaltenes removed from the suspension by centrifugation. Prior to hydropyrolysis both samples were loaded with the Mo catalyst as previously described (Snape et al., 1989; Lafferty et al., 1993; Roberts et al., 1995) with an aqueous/methanol solution of ammonium dioxydithiomolybdate [$(NH_4)_2MoO_2S_2$] to give a nominal molybdenum loading of 1 wt.% sample. The asphaltenes were also mixed (1:1 w/w) with acid washed (dilute HCl) and pre-extracted (DCM/methanol) sand.

2.2. Catalytic fixed bed hydropyrolysis

Fixed bed hydropyrolysis of the samples was conducted using the apparatus and procedure described in detail elsewhere (Snape et al., 1989; Lafferty et al., 1993; Love et al., 1995). Briefly, the samples were pyrolysed with resistive heating from 50 to 250 °C at 300 °C min^{-1}, and then from 250 to 500 °C at 8 °C min^{-1}, under a hydrogen pressure of 15 MPa. A hydrogen sweep gas flow of 10 dm^3 min^{-1}, measured at ambient temperature and pressure, ensured that the products were quickly removed from the reactor vessel. As in previous studies, the hydropyrolysates were recovered with multiple washes of DCM from the dry ice cooled trap, which consisted of coils of 3/8″ stainless steel (Fig. 1A). These results could then be compared with those obtained with the hydropyrolysates collected in the silica filled trap (Fig. 1B) constructed from 1/4″ stainless steel (0.180″ i.d.), and designed to hold approximately 1 g of silica. To ensure that there was no contamination of the products, the silica used for trapping (35–70 mesh) was pre-extracted in a soxhlet apparatus with *n*-hexane for 24 h and DCM/methanol (93:7 v/v) for 48 h, and dried in a baffle furnace at 600 °C for 4 h.

2.3. Whole oil recovery

In order to quantitatively assess the recovery of hydrocarbons by hydropyrolysis, aliquots (~50 mg) of a light crude oil were adsorbed to a small amount of silica and pyrolysed. The desorbed oils were recovered from each of the two designs of trap and cooled by both dry ice and liquid nitrogen. The temperature within the silica trap was measured by inserting a thermocouple into the trap at the base of the silica column during a blank run with each of the two coolants. Quantification of the recovered hydrocarbons (DCM soluble fraction) was achieved by the addition of squalane, with analysis by gas chromatography–flame ionisation detection (GC–FID), performed on a Chromopack CP9001 instrument, with separation achieved on a fused silica capillary column (25 m×0.22 mm i.d.) coated with BPX5 phase (0.25 μm thickness). Helium was employed as the carrier gas, with a temperature programme of 50 °C (2 min) to 300 °C (14 min) at 5 °C min^{-1}.

2.4. Hydopyrolysis product analysis

The aliphatic, aromatic and polar (NSO) fractions of the oil shale and asphaltene hydropyrolysates were separated by silica gel adsorption chromatography with successive elutions of *n*-hexane, *n*-hexane/DCM (4:1 v/v) and DCM/methanol (1:1 v/v). The yields of each fraction were determined by evaporation under a stream of dry nitrogen in pre-weighed vials. In order to assess the degree of carbon conversion during hydropyrolysis, and the yield of carbon recovered, the carbon content (wt.%) of the samples, pyrolysis residues, silica trapped hydropyrolysates and desorption residues was determined using a UCI Coulometrics CO_2 coulometer. The

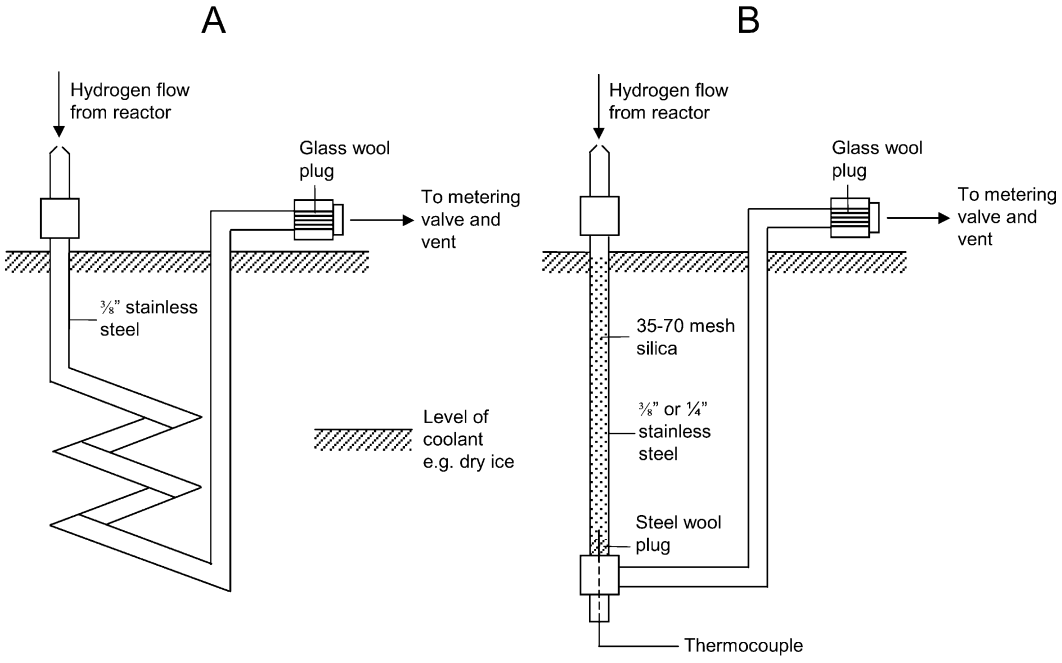

Fig. 1. Schematic representation of the traps used for the recovery of the hydropyrolysates: A—coiled steel trap; B—silica filled trap.

errors for measuring these conversions are estimated at ±5%, based on previously described repeat analyses (Love et al., 1995).

GC–MS analyses of the fractionated samples (1 μl in DCM) were performed on a Fisons Instruments 8000 gas chromatograph interfaced to a MD 800 mass spectrometer (ionising energy 70 eV, source temperature 280 °C). Separation was performed on a column similar to that used for the GC analyses, with helium as the carrier gas and an oven programme of 50 °C (2 min) to 300 °C (28 min) at 5 °C min^{-1}. The selected ions monitored included m/z 83 (*n*-alk-1-enes), m/z 85 (*n*-alkanes), m/z 191 (hopanes) and m/z 217 (steranes). The addition of standard 5β(H)-cholane (Chiron, Trondheim) to the aliphatic fraction prior to GC–MS analysis allowed quantification of individual compounds, assuming a response factor of one (Love et al., 1995, 1996). In addition to the characterisation of the biomarkers released during hydropyrolysis, the compositional distribution of these products throughout the silica column was also investigated. The silica recovered from the trap was split into 4 sections relative to the position in the column, and these sections were analysed for their hydrocarbon distribution and carbon content (wt.%) as described above.

2.5. Thermal desorption of hydropyrolysates

The off-line thermal desorption of the silica-trapped hydropyrolysates of GOS were performed in the hydropyrolysis reactor under an atmospheric pressure of hydrogen with a sweep gas flow of 100 cm^3 min^{-1}, measured at ambient temperature. The samples were desorbed with a heating rate of 50–300 °C at 300 °C min^{-1}, with the final temperature held for 2 min. Further tests were carried out to a maximum temperature of 350, 400, 450 and 500 °C, at the same heating rate, with the final temperature again held for 2 min. The desorbed products were recovered after trapping on silica as for the hydropyrolysis experiments, with the distribution of hydrocarbons recovered compared with the original hydropyrolysate to establish whether secondary cracking or configurational alteration of the biomarkers was significant during desorption.

The on-line thermal desorption-GC–MS of the silica-trapped hydropyrolysates was performed using a CDS 1000 pyroprobe, platinum heated filament, pyrolyser (Chemical Data System, Oxford, USA) directly connected to a Varian 3400 gas chromatograph coupled to a Varian Saturn II ion trap mass spectrometer. The py/GC interface and the split/splitless Varian 1077 injector (at split ratio 30:1) were kept at 280 °C. Separation was performed on a Supelco MDN-5S capillary column (30 m×0.25 mm i.d., 0.25 μm film thickness) with a temperature programme from 50 °C (2 min) to 310 °C (16 min) at 5 °C/min, using helium as carrier gas. Mass spectra were recorded in the electron ionisation mode (70 eV) at 1 scan/sec, mass range 45–550 m/z, filament current at 10 μA, ion trap at 200 °C. The silica-trapped hydropyrolysate (about 5 mg) and neat Göynük hydropyrolysate (about 0.2 mg) were pyrolysed at 700 °C (set temperature) for 10 s at the maximum heating rate. For comparison with the generated pyrolysate, a solution containing the aliphatic fraction of the GOS hydropyrolysate was analysed by GC–MS, using the conditions described above.

3. Results and discussion

3.1. Hydropyrolysate recovery

The recovery of the light crude oil by desorption in the hydropyrolysis rig is illustrated in Fig. 2. The gas chromatogram of the oil (Fig. 2A) is dominated by a homologous series of *n*-alkanes (*n*-C_7–*n*-C_{32}) and low molecular mass (MM) aromatic compounds such as benzene and toluene. Table 1 indicates the recovery of these compounds for the two types of trap, using the different coolants. For the relatively high MM alkanes (>*n*-C_{10}), both traps are efficient (generally recovery >80% w/w), with no significant difference between the two coolants. Major differences in recovery are only apparent for the relatively low MM compounds (<*n*-C_{10}), and so the trapping efficiency of biomarker hydrocarbons (>*n*-C_{20}) would be equally as good for the silica trap as for the coiled steel design. Therefore, the recovered oil fractions (Fig. 2B and C) are illustrated as partial gas chromatograms showing only the distribution of the low MM compounds.

Table 1
Recovery (% w/w) of selected hydrocarbons desorbed from a light crude oil under hydropyrolysis conditions, with dry ice and liquid nitrogen used as the coolant

Compd	Boiling point (°C)	Coiled trap		Silica trap	
		Liquid N_2	Dry ice	Liquid N_2	Dry ice
Benzene	80	58	0	43	0
n-C_7	98	58	0	46	0
Toluene	110	83	52	83	37
n-C_8	126	79	51	77	4
n-C_9	151	83	75	85	84
n-C_{10}	174	87	83	97	88
n-C_{11}	196	89	87	96	89
n-C_{12}	216	89	88	91	91
n-C_{13}	235	91	90	87	94
n-C_{14}	254	97	95	99	98
n-C_{15}	271	96	93	102	96
n-C_{20}	343	86	88	92	92
n-C_{25}	402	81	85	78	89
n-C_{30}	450	77	94	81	88

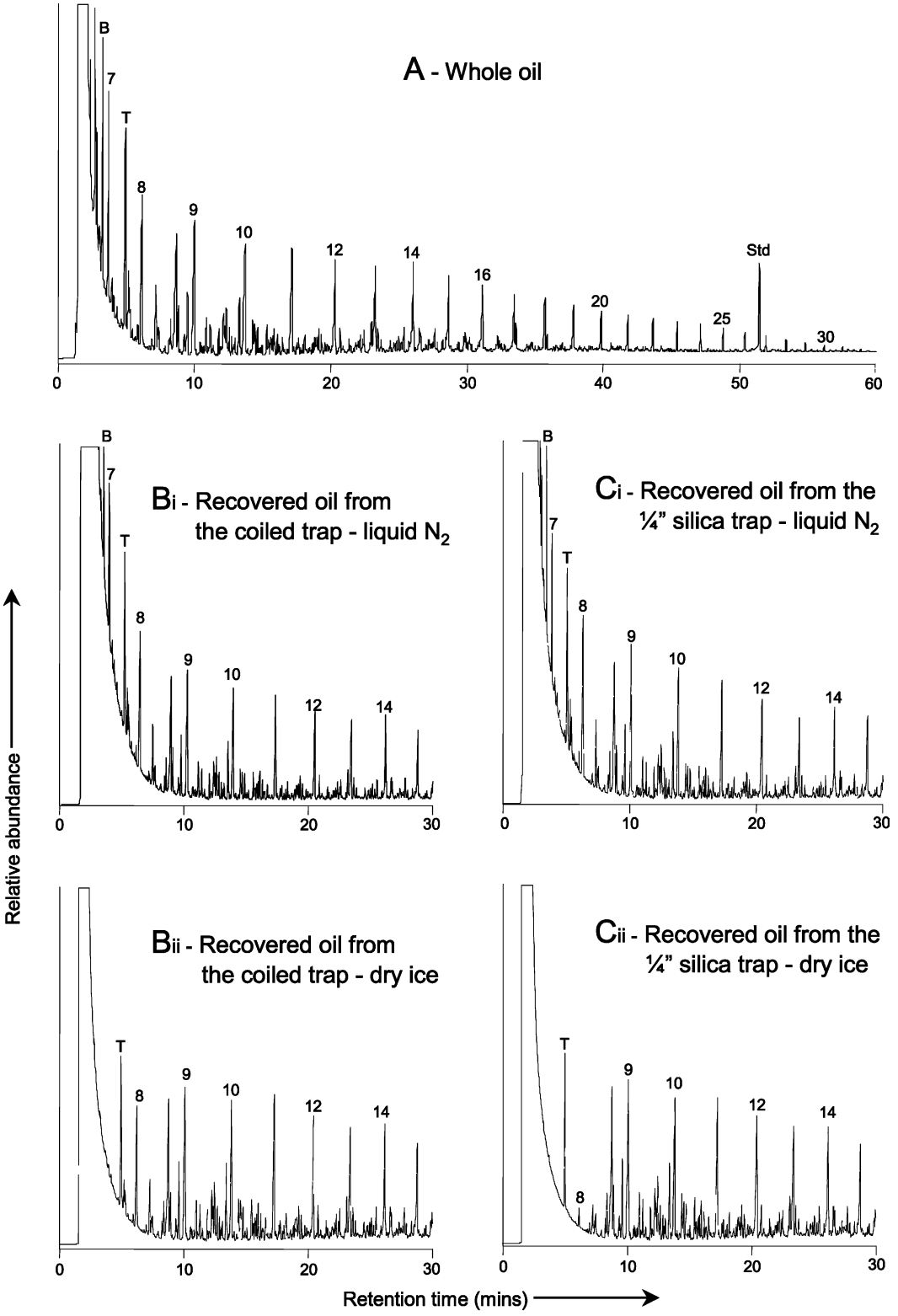

Fig. 2. Comparison of the whole oil gas chromatogram (A), and the partial gas chromatograms of the DCM-soluble fraction desorbed by the hydropyrolysis of a light crude oil, with trapping by the coiled steel (B) and silica filled traps (C), cooled by liquid nitrogen (i) and dry ice (ii). Numbers refer to the carbon number of the *n*-alkanes; B—Benzene; T—toluene; Std—squalane.

The use of liquid nitrogen as the coolant in place of dry ice resulted in a significantly enhanced recovery of low MM compounds such as *n*-heptane and *n*-octane, benzene and toluene. The recovery of these hydrocarbons was slightly greater from the coiled steel trap cooled with liquid nitrogen than from the silica-filled trap. The higher recovery from the coiled steel trap was more significant with dry ice as the coolant, for example with 37% w/w of the toluene recovered from silica trap, compared with 52% w/w from the coiled steel trap.

The efficiency of trapping the desorbed hydrocarbons will be largely dependent on the temperature within the trap during the course of the 40-min hydropyrolysis run. This will be controlled by the extent to which hydrogen cools as it is swept out of the reactor, the volume of gas passing through the trap and the efficiency of the coolant. The temperature and volume of the sweep gas have been optimised in previous studies to maximise the yield of biomarkers whilst minimising structural alteration (Love et al., 1997). Obviously, due to its much lower temperature (−196 °C), the liquid nitrogen should be a much more efficient coolant than the solid dry ice (−78 °C). However, the liquid nitrogen tended to quickly evaporate during the course of the run as the hot sweep gas warmed the trap. Therefore, as shown in Fig. 3, the temperature of the trap rose steadily from −130 °C when the reactor was at 300 °C, to 85 °C at the end of the test. This is similar to the final temperature observed when dry ice was used as the coolant, and might have caused some of the low MM compounds to evaporate and be swept out of the trap. In order to minimise this temperature increase, a method would need to be devised by which the liquid nitrogen lost to evaporation could be continually replenished, to ensure that the trap was always fully submerged.

These results demonstrate the relatively high efficiency of both designs of trap for the recovery of hydrocarbons desorbed by hydropyrolysis. The silica trap method, with important advantages of decreased experimental turn-around time, and reduced sample handling, produced data comparable to those from the coiled steel trap. Of the two coolant methods, dry ice is the more convenient to use and so, unless the target compounds of an experiment are relatively volatile, there is no significant advantage in using liquid nitrogen.

3.2. Hydropyrolysis of the Göynük oil shale

Information on the efficiency of the different designs of trap in recovering the hydropyrolysate generated from the GOS is presented in Table 2. As in previous studies on this shale, hydropyrolysis resulted in carbon conversions of >90%, with relatively high yields of the GC amenable aliphatic and aromatic hydrocarbons generated. The efficiencies of the traps are expressed as the% of the converted carbon, and the wt.% of the total products recovered in each type (Table 2), these indicate that the silica-filled and coiled steel traps recover similar proportions of the converted organic carbon, principally as DCM-soluble products. The recoveries may be slightly underestimated due to evaporative losses, which are inevitable while removing the excess DCM to obtain the total hydropyrolysate yield.

The distribution of the GOS hydropyrolysate throughout the trapping silica column is presented in

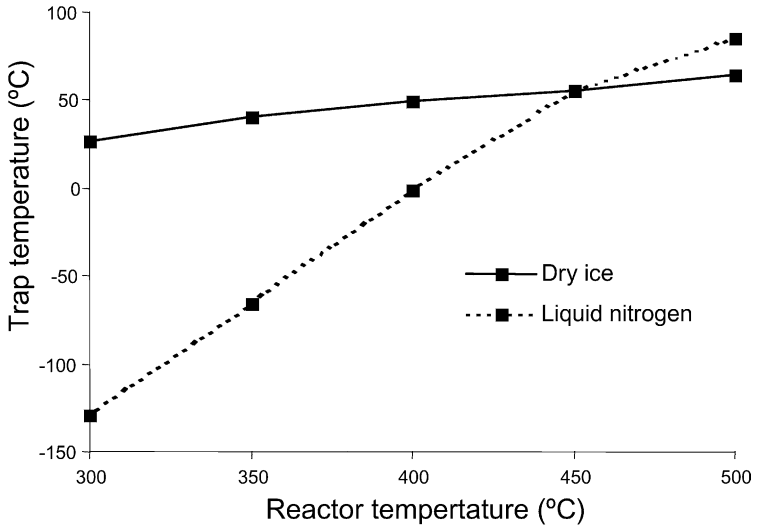

Fig. 3. Temperature profile of the silica trap during hydropyrolysis experiments.

Table 2
Comparison of the results obtained from the hydropyrolysis of Göynük oil shale and Soldado crude oil asphaltenes, with the coiled and silica trapping methods

	Göynük oil shale		Soldado asphaltene	
	Coiled	Silica	Coiled	Silica
Sample weight (mg)	100	50	50	50
Trap silica weight (g)	–	1	–	1
Carbon conversion (% initial TOC)[a]	91	93	72	72
Trapping efficiency (% TOC generated)[b]	92	95	56	54
Trapping efficiency (wt.% of products)[c]	80	81	42	41
Yield of aliphatics (mg/g initial TOC)[d]	159	175	151	134
Yield of aromatics (mg/g initial TOC)[e]	89	101	103	114
Yield of total oil (mg/g initial TOC)[f]	1111	1199	486	474

[a] % TOC removed from sample by hydropyrolysis.
[b] % Of generated TOC recovered from trap.
[c] % Of sample weight loss recovered as DCM soluble product oil.
[d] Weight of recovered aliphatic fraction (mg)/weight of initial TOC (g).
[e] Weight of recovered aromatic fraction (mg)/weight of initial TOC (g).
[f] Total weight of recovered DCM soluble product oil (mg)/weight of initial TOC (g).

Table 3. The results for each section are expressed as the wt.% of each fraction present, together with the proportion of carbon recovered. The vast majority of the hydropyrolysate is adsorbed to the upper quarter section, with $>70\%$ w/w of each fraction and of the total carbon, in this section. There is then a rapid decrease in the proportion of hydropyrolysate adsorbed moving to the middle sections, with $<5\%$ w/w present in the lower section. These results suggest that, providing sufficient silica is present in the trap for the mass of carbon generated, no significant quantities of the product, other than highly volatile compounds, should pass through the trap without being adsorbed to the silica.

In addition to the total yield of hydropyrolysate recovered, it is also important that the silica-filled trap produces biomarker hydrocarbon profiles similar to those obtained from the coiled steel trap. A number of maturity dependent biomarker ratios based on the abundance of individual isomers are listed in Table 4, these indicate that the composition of the hydropyrolysate recovered from the silica-filled trap is very similar to that from the coiled steel trap. In addition, it can be seen that the top section of the silica column, which as described contains the highest concentration of hydropyrolysate, is representative of the silica column as a whole. This has implications for the on-line thermal desorption-GC–MS of the silica-trapped hydropyrolysate described below, as only a small amount of the total silica recovered from the trap can be introduced to the pyroprobe at any one time.

Table 3
Distribution of the hydropyrolysate for Göynük oil shale (wt.%) and TOC (%) throughout the silica trap

Silica section	% Aliphatic	% Aromatic	% Polar	% TOC
Upper	80	71	70	73
Upper middle	13	16	18	15
Lower middle	5	8	7	8
Lower	2	5	5	4

3.3. Hydropyrolysis of oil asphaltenes

The recovery and product composition obtained from hydropyrolysis of the asphaltene fraction isolated from Soldado crude oil are presented in Table 2. A total conversion of 72% of the initial organic carbon to organic products and gas was obtained; again, these results highlight the comparability of the two designs of trap. The recovery of the hydropyrolysate was significantly lower than that seen with the oil shale, with approximately 55% of the generated carbon and 40% of the total products (by weight) recovered from both types of trap. The low conversion and recovery resulted in a reduced yield of approaching 50% w/w of DCM soluble products relative to the mass of initial carbon, suggesting that large quantities of gaseous and volatile liquids were also generated. A conversion significantly lower than that seen with the GOS might be due to the composition and higher maturity of the asphaltenes, which contain a high proportion of polar compounds. However, the results from the hydropyrolysis of carboxylic acids adsorbed to silica (to be published in a subsequent paper) suggest that a low conversion may result from interaction between the sorbant and the highly polar carbonyl functional groups, resulting in greater amounts of unconverted residue (cf. Park et al.,

2000). Although the sand mixed with the asphaltenes in these experiments will have a lower surface area than fine grained silica, such adsorption effects may have inhibited conversion.

The aliphatic hydrocarbon biomarker ratios presented in Table 5 indicate that the thermal maturity of the bound biomarkers released from the asphaltene fraction are significantly lower than with the free hydrocarbon components. Such retarded maturity of bound biomarkers in relation to those in the free phase is well established, having been previously reported for the pyrolysates of asphaltenes (Murray et al., 1999), source rock kerogens (Seifert, 1978; Murray et al., 1998) and coals (Mykce and Michaelis, 1986; Michaelis et al., 1989; Love et al., 1996) and is believed to result from the steric protection afforded to the biomarkers when covalently-bound within the structure of geomacromolecules (Love et al., 1995).

3.4. Off-line thermal desorption of silica-trapped hydropyrolysis products

The yields recovered from the off-line thermal desorption pyrolysis of the silica-trapped hydropyrolysates are presented in Fig. 4. Although the total yield of products desorbed at all temperatures is significantly lower than the amount of the starting hydropyrolysate, the effect of temperature is apparent, with a steady increase in the recovery of the aliphatic, aromatic and polar fractions from a final temperature of 300 °C through to 500 °C. The yield of aliphatics at 500 °C is similar to that in the original hydropyrolysate, with the reduction in overall yield due to the poor recovery of the aromatic and polar fractions.

Analysis of the desorption residues indicate that a significant proportion of the carbon in the hydropyrolysate from oil shale was not desorbed from the

Table 4
Selected aliphatic biomarker maturity parameters for the Göynük oil shale hydropyrolysate

Ratio	Coiled trap	Silica trap	
		All silica	Upper section
C_{31} αβ (22S/S + R)[a]	0.21	0.18	0.18
C_{32} αβ (22S/S + R)[b]	0.14	0.12	0.14
C_{30} βα/αβ[c]	1.97	2.03	2.02
Ts/Tm[d]	0.29	0.29	0.32
C_{29} ααα (20S/S + R)[e]	0.05	0.05	0.05
C_{29} αββ/ααα + αββ[f]	0.27	0.25	0.27

[a] αβ-homohopane 22S/S + R-starting value 0, ratios reach end point at 0.6 before the onset of intense oil generation.
[b] C_{32} αβ-dihomohopane 22S/S + R-as ratio [a].
[c] C_{30} βα-moretane/C_{30} αβ-hopane—ratio decreases with increasing maturity.
[d] 18α,21β?(H)-22,29,30-trisnorneohopane/17α,21β(H)-22,29,30-trisnorhopane—ratio increases with increasing maturity.
[e] C_{29} ααα-ethylcholestane 20S/S + R-starting value 0, increases to 0.5 with increasing maturity.
[f] C_{29} ethylcholestane αββ/ααα + αββ-starting value 0, increases to 0.8 with increasing maturity.

Table 5
Selected aliphatic biomarker maturity parameters obtained from hydropyrolysis of the Soldado crude oil asphaltenes

Ratio	Crude oil	Asphaltene HyPy product	
		Coiled trap	Silica trap
C_{31} αβ (22S/S + R)[a]	0.53	0.44	0.44
C_{32} αβ (22S/S + R)[b]	0.53	0.45	0.45
C_{30} βα/αβ[c]	0.14	0.21	0.21
Ts/Tm[d]	0.47	0.09	0.10
C_{29} ααα (20S/S + R)[e]	0.53	0.19	0.21
C_{29} αββ/ααα + αββ[f]	0.66	0.40	0.38

[a] αβ-Homohopane 22S/S + R-starting value 0, ratios reach end point at 0.6 before the onset of intense oil generation.
[b] C_{32} αβ-dihomohopane 22S/S + R-as ratio [a].
[c] C_{30} βα-moretane/C_{30} αβ-hopane—ratio decreases with increasing maturity.
[d] 18α,21β?(H)-22,29,30-trisnorneohopane/17α,21β(H)-22,29,30-trisnorhopane—ratio increases with increasing maturity.
[e] C_{29} ααα-ethylcholestane 20S/S + R-starting value 0, increases to 0.5 with increasing maturity.
[f] C_{29} ethylcholestane αββ/ααα + αββ-starting value 0, increases to 0.8 with increasing maturity.

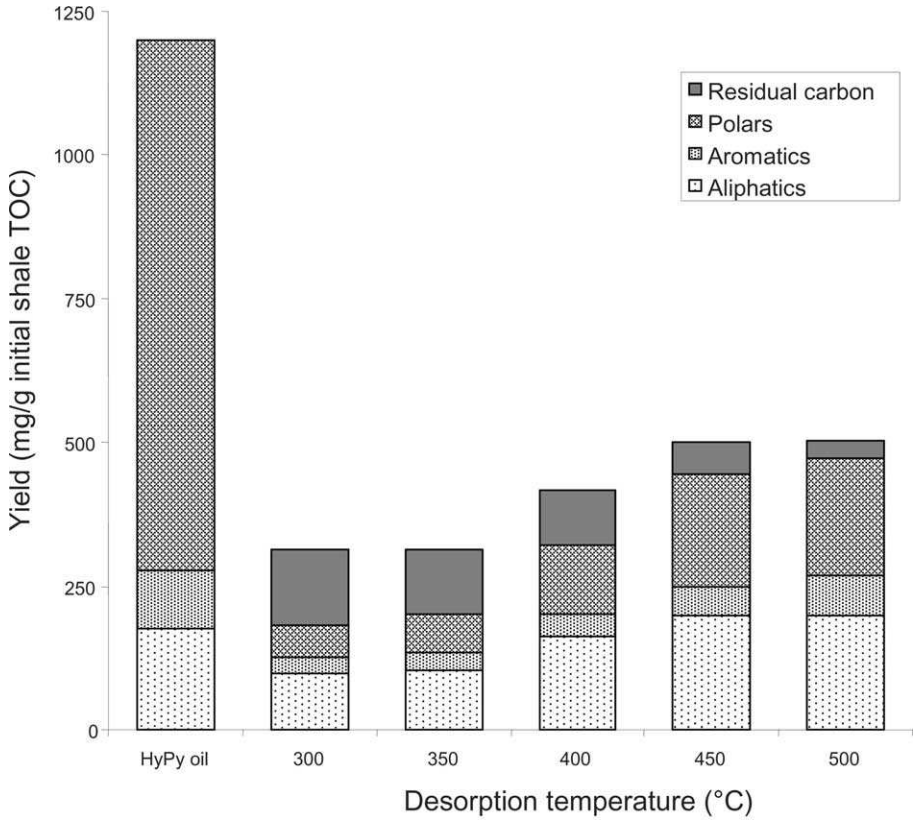

Fig. 4. Yield (mg/g initial shale TOC) of aliphatic, aromatic and polar fractions in the thermally desorbed (off-line) Göynük oil shale hydropyrolysates compared to the original hydropyrolysate.

trapping silica (131 mg/g initial shale TOC at 300 °C; 33 mg/g initial shale TOC at 500 °C), although when this is added to the yield of desorbed DCM soluble products, there is clearly an overall loss of ca. 50% of the starting carbon at 500 °C. As noted for the reduced yield of asphaltenes during hydropyrolysis, interactions between the silica sorbant and polar functional groups in the sample may result in the reduced desorption of this fraction relative to the non-polar aliphatics and aromatics. However, the low recovery could be a result of the polar material condensing in the non-heated zone of the reactor; this is being further investigated.

The distribution of aliphatic hydrocarbons in the hydropyrolysate from the GOS (Fig. 5A) is dominated by a bimodal distribution of *n*-alkane/*n*-alk-1-ene doublets (maximum at C_{30} and sub-maximum at C_{21}), with the homologous series extending up to C_{40} (cf. Love et al., 1995). The *n*-alkanes are the more abundant, with an even-over-odd predominance (EOP) apparent among the longer-chain homologues and the distribution of *n*-alk-1-enes mirroring that of their saturated analogues. Such doublets are ubiquitous components of kerogen pyrolysates (Larter and Horsfield, 1993), although as noted by Love et al. (1995), the survival of *n*-alkanes heavier than $\sim C_{35}$ is not often observed in on-line pyrolysis experiments (e.g. Derenne et al., 1988). As shown in Fig. 5B, with desorption at 300 °C, the higher MM alkanes are clearly not desorbed efficiently as the *n*-alkane/*n*-alk-1-ene doublet envelope has a different shape and a maximum abundance at C_{16}. However, with desorption at 500 °C (Fig. 5D) the profile is very similar to that of the original hydropyrolysate.

Changes in these profiles with increasing desorption temperature can be assessed by measuring the ratio in abundance between a long-chain alkane e.g. *n*-C_{30} and a relatively short-chain compound, which would not be subject to evaporative losses e.g. *n*-C_{18}. This parameter may also vary as a result of cracking of the longer chain *n*-alkanes, which could potentially arise at higher desorption temperatures, resulting in a concurrent increase in the abundance of the shorter-chain homologues (Kissin, 1987). Secondary cracking during both hydropyrolysis and subsequent thermal desorption would also result in a decrease in the magnitude of the EOP amongst the longer-chain *n*-alkanes (Love et al., 1997), which can be assessed by the carbon preference index (CPI; formula of Philippi, 1965), and lead to an increase in the abundance of the unsaturated *n*-alk-1-enes in these samples

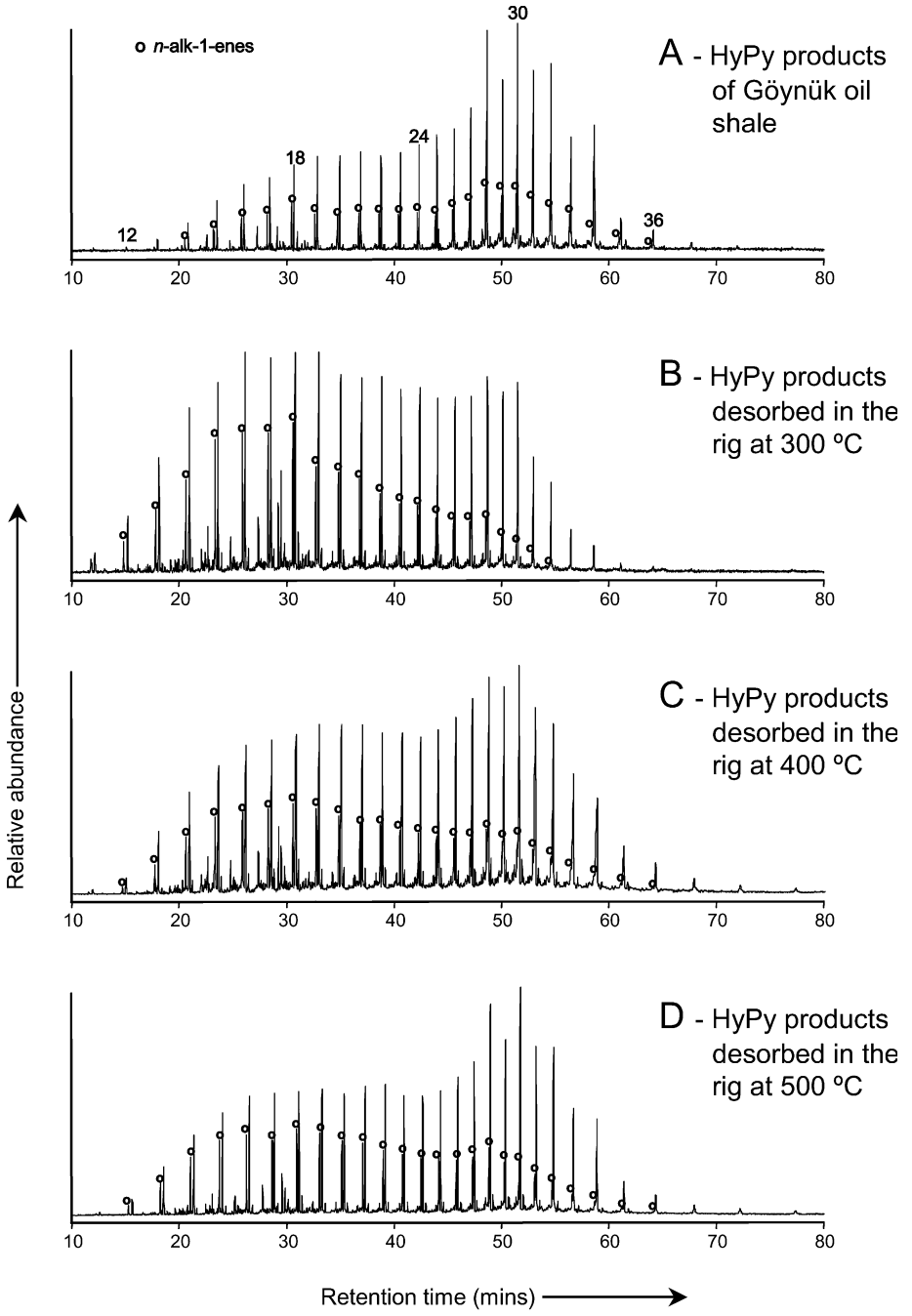

Fig. 5. Total ion chromatogram of the aliphatic components in the thermally desorbed (off-line) Göynük oil shale hydropyrolysates compared to the original hydropyrolysate. Numbers refer to the carbon number of the *n*-alkanes.

relative to the *n*-alkanes (Behar and Pelet, 1984; Van Lieshout et al., 1997). These ratios for each desorption temperature are listed in Table 6 and suggest that, with the exception of the poorly desorbed 300 °C sample and some evidence of minor cracking at higher temperature, the *n*-alkane distributions in the desorbed oils are not that dissimilar to that of the original hydropyrolysate.

Fig. 6 compares the distribution of the hopane and sterane biomarkers present in the original hydropyrolysate and those recovered from its off-line desorption at 300, 400 and 500 °C. The peak assignments for

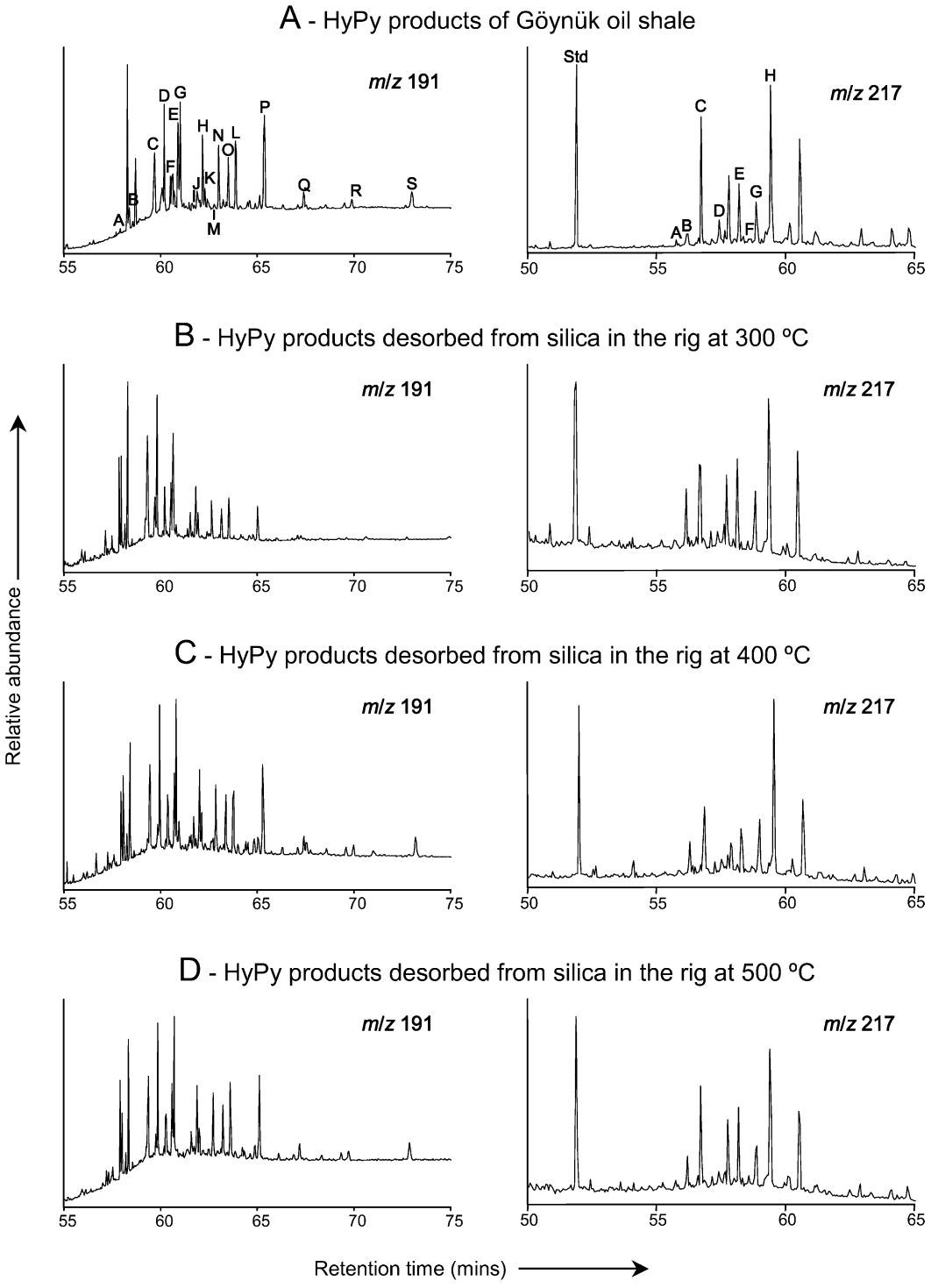

Fig. 6. Partial mass chromatograms showing distributions of selected aliphatic biomarker hydrocarbons (m/z 191 for hopanes; m/z 217 for steranes) in the thermally desorbed (off-line) Göynük oil shale hydropyrolysates compared to the original hydropyrolysate. For peak assignments see Table 7.

these fragmentograms, together with the concentration of the individual biomarker compounds desorbed at each temperature, are listed in Table 7. Although the maturity dependent biomarker ratios for the original hydropyrolysate are fairly consistent with those for the desorbed oils for all temperatures (Table 8), these parameters are all based on the abundance of various compounds of a similar carbon number having similar boiling points. Therefore, they are not greatly affected by the differential recoveries as a function of boiling point at lower desorption temperatures. The hydropyrolysate desorbed at 300 °C (Fig. 6B) can be seen to contain a very low concentration of hopanes $>C_{32}$, despite having an apparently "normal" distribution

Table 6
Molecular abundance ratios to monitor secondary cracking during the thermal desorption of the silica trapped hydropyrolysate for Göynük oil shale

Desorption temperature (°C)	n-C_{18}/n-C_{30} alkane	CPI[a]	Total alkanes/alk-1-enes
300	1.21	0.71	0.36
350	0.50	0.83	0.33
400	0.50	0.83	0.33
450	0.50	0.83	0.34
500	0.50	0.82	0.37
HyPy oil	0.33	0.79	0.30

[a] CPI after Philippi (1965) = $2*C_{29}/(C_{28}+C_{30})$.

Table 7
Yield (μg/g initial TOC) and peak assignments of selected hopanes and steranes from the hydropyrolysate of the Göynük oil shale and the desorbed oil of this product

	Peak	HyPy oil	Desorption temp. (°C)				
			300	350	400	450	500
Hopane							
18α,21β(H)-22,29,30-trisnorneohopane (Ts)	A	5	3	8	10	6	8
17α,21β(H)-22,29,30-trisnorhopane (Tm)	B	18	14	28	31	26	31
17α,21β(H)-30-norhopane	C	69	27	43	52	47	73
17β,21α(H)-30-normoretane	D	59	22	46	52	53	61
17β,21β(H)-30-norhopane	E	58	10	36	34	41	38
17α,21β(H)-hopane	F	35	10	25	28	27	29
17β,21α(H)-moretane	G	72	20	50	53	57	59
17β,21β(H)-hopane	H	53	10	33	35	38	41
17α,21β(H)-homohopane (22S)	I	4	1	3	4	4	5
17α,21β(H)-homohopane (22R)	J	17	5	12	15	15	17
17β,21α(H)-homomoretane	K	16	5	15	14	16	20
17β,21β(H)-homohopane	L	67	10	37	41	44	48
17α,21β(H)-dihomohopane (22S)	M	6	1	4	5	4	6
17α,21β(H)-dihomohopane (22R)	N	52	8	32	33	34	39
17β,21α(H)-dihomohopane	O	36	7	25	28	35	34
17β,21β(H)-dihomohopane	P	97	9	49	54	55	64
17β,21β(H)-trihomohopane	Q	18	2	10	13	14	14
17β,21β(H)-tetrahomohopane	R	14	1	8	10	10	12
17β,21β(H)-pentahomohopane	S	28	1	15	21	21	25
Sterane							
5α,14α,17α(H)-cholestane (20S)	A	2	1	2	2	2	2
5β,14α,17α(H)-cholestane (20R)	B	6	3	6	6	6	6
5α,14α,17α(H)-cholestane (20R)	C	21	8	15	16	19	19
5α,14α,17α(H)-24-methylcholestane (20S)	D	1	1	2	2	2	2
5α,14α,17α(H)-24-methylcholestane (20R)	E	11	5	11	10	12	14
5α,14α,17α(H)-24-ethylcholestane (20S)	F	1	1	1	1	2	1
5β,14α,17α(H)-24-ethylcholestane (20R)	G	11	5	10	12	11	12
5α,14α,17α(H)-24-ethylcholestane (20R)	H	36	13	30	32	31	37

(although greatly reduced concentration) of C_{30}, C_{31} and C_{32} compounds. The yields of total hopanes and steranes recovered by thermal desorption are summarised in Fig. 7 which demonstrates the inefficency of the desorption of these relatively high MM components at the lower temperatures used, while emphasising their very high (>80%) recovery at a desorption temperature of 500 °C (Fig. 6D). These results further confirm the very high recoveries of aliphatics suggested in Fig. 4.

In addition to high recoveries, it is important that these biomarker compounds do not undergo any structural rearrangement during desorption. Higher MM extended (C_{33}–C_{35}) hopanes with the thermodynamically unstable 17β(H),21β(H) stereochemistry are most susceptible to isomerisation and/or cracking of the alkyl side chain (Love et al., 1997). The high abundance of these compounds (peaks Q, R and S in Fig. 6) in the desorption products at 450 and 500 °C suggest that this regime does not lead to significant structural rearrangement of the hydropyrolysis products, resulting in a biomarker profile that is representative of the original kerogen. As reported by Love et al. (1997), the sterane products generated by hydropyrolysis of the GOS are dominated by those usually associated with immature geological settings, especially epimers with the 5α(H),14α(H),17α(H) and 20R configurations. This distribution is repeated amongst all of the desorbed oils, and there is no evidence of the isomerisation of these compounds to the more thermodynamically stable 5α(H),14α(H),17α(H) 20S epimers (for ratios see Table 8). However, since isomerisation of steranes (at C-20) is known to occur more slowly than that for hopanes (Mackenzie, 1984), the steranes can be expected to be less sensitive indicators of product rearrangement

Table 8
Selected aliphatic biomarker maturity parameters for the Göynük oil shale hydropyrolysate, and the thermally desorbed oils from this product

Ratio	HyPy oil	Desorption temperature of HyPy oil (°C)				
		300	350	400	450	500
C_{31} αβ S/S + R[a]	0.19	0.19	0.19	0.23	0.24	0.22
C_{32} αβ S/S + R[b]	0.10	0.14	0.12	0.14	0.12	0.14
C_{30} βα/αβ[c]	2.08	2.01	1.99	1.94	2.09	2.03
Ts/Tm[d]	0.29	0.23	0.27	0.30	0.25	0.27
C_{29} ααα S/S + R[e]	0.03	0.04	0.04	0.03	0.05	0.03
C_{29} αββ/ααα + αββ[f]	0.24	0.29	0.27	0.27	0.28	0.26

[a] αβ-homohopane 22S/S + R- starting value 0, ratios reach end point at 0.6 before the onset of intense oil generation.
[b] C_{32} αβ-dihomohopane 22S/S + R-as ratio [a].
[c] C_{30} βα-moretane/C_{30} αβ-hopane—ratio decreases with increasing maturity.
[d] 18α,21β(H)-22,29,30-trisnorneohopane/17α,21β(H)-22,29,30-trisnorhopane—ratio increases with increasing maturity.
[e] C_{29} ααα-ethylcholestane 20S/S + R starting value 0, increases to 0.5 with increasing maturity.
[f] C_{29} ethylcholestane αββ/ααα + αββ-starting value 0, increases to 0.8 with increasing maturity.

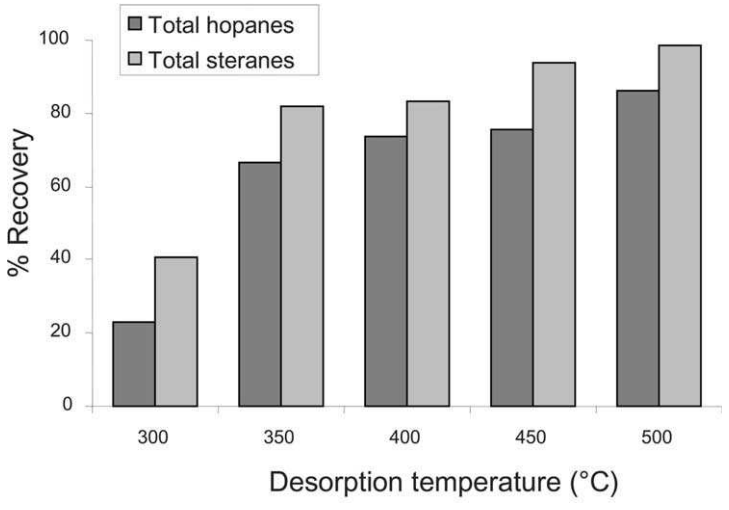

Fig. 7. Total yield (%) of hopanes and steranes recovered by the off-line thermal desorption of the GOS hydropyrolysate.

than the hopanes during both the hydropyrolysis and thermal desorption stages.

Further refinement of the heating programme in terms of both rate and the final temperature reached in the off-line desorption system is necessary to maximise the yield of aromatic and polar material. Such refinements could be accomplished by the on-line thermal desorption of silica-trapped hydropyrolysates with a simple programmed temperature vaporiser (PVT) injector, with a capacity for gram quantity samples and cryogenic focussing, such as that described by van Lieshout et al. (1996, 1997). Alternatively, it could be possible to link the hydropyrolysis apparatus directly to a GC or GC–MS by fitting a heating system to the silica trap in order to desorb the products as soon as the hydropyrolysis run finished. However, this would require a system of heated transfer lines and valves between the trap and the instrument interface, which could contain cold spots, resulting in the loss of high molecular mass components. Either system would allow complete hydropyrolysis and characterisation of samples in around 2 h.

3.5. On-line thermal desorption of silica-trapped hydropyrolysis products

The on-line thermal desorption of the silica-trapped GOS hydropyrolysate (Fig. 8) resulted in greater evidence of secondary cracking than was apparent in the off-line studies. In comparison to the aliphatic fraction of the original GOS hydropyrolysate (Fig. 8A), the products generated by the on-line desorption of the silica-trapped hydropyrolysate (Fig. 8C) contained a significantly greater proportion of the shorter-chain *n*-alk-1-enes (n-C_{10}–n-C_{15}). Furthermore, the envelope of *n*-alkanes showed a different pattern, with, in addition to

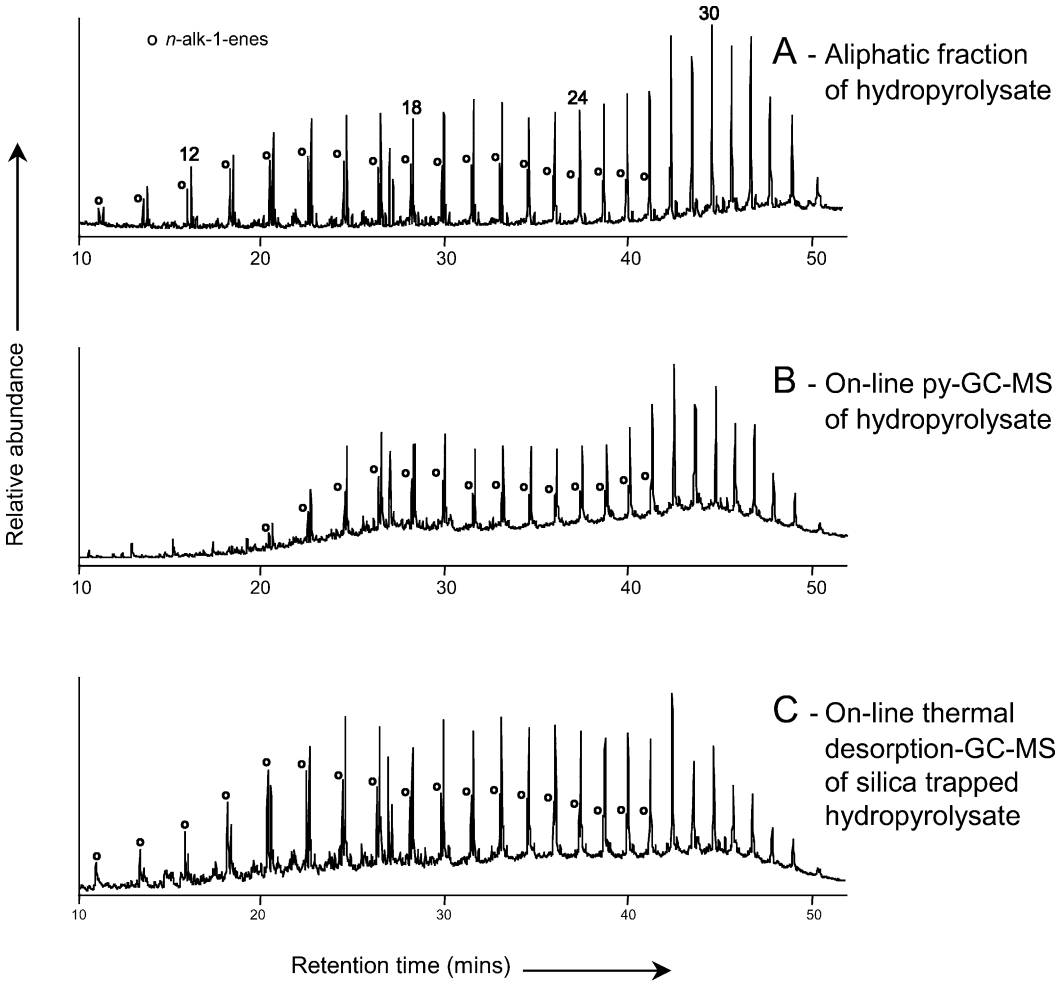

Fig. 8. Total ion chromatogram of the aliphatic hydrocarbon fraction of the Göynük oil shale hydropyrolysate (A), compared to the on-line py-GC–MS of the Göynük oil shale hydropyrolysate (B), and the on-line thermal desorption-GC–MS of the silica trapped Göynük oil shale hydropyrolysate (C). Numbers refer to the carbon number of the *n*-alkanes.

the higher relative abundance of shorter-chain *n*-alkanes, the maximum in abundance was at *n*-C_{28} instead of *n*-C_{30}, and fewer of the very long-chain homologues were apparent. Fig. 9 shows the comparison between the hopane (up to and including C_{33}), and sterane distributions in the original hydropyrolysate (Fig. 9A), those obtained by the on-line py-GC–MS of the neat hydropyrolysate (Fig. 9B) and those generated from the thermal desorption-GC–MS of the silica trapped hydropyrolysate. As with the off-line studies, the recovery of high MM extended hopanes and steranes with the biologically inherited and thermodynamically unstable stereochemistry, which would be the most susceptible to isomerisation and/or cracking of the alkyl side chain (Love et al., 1997), suggests that the degree of cracking is not too extensive. However, a more concentrated loading of silica-trapped hydropyrolysate than that used here is required to give better sensitivity for the steranes and hopanes.

Figs. 8 and 9 also show that, with the exception of low MM compounds that were lost during product work-up, the on-line thermal desorption-GC–MS of the

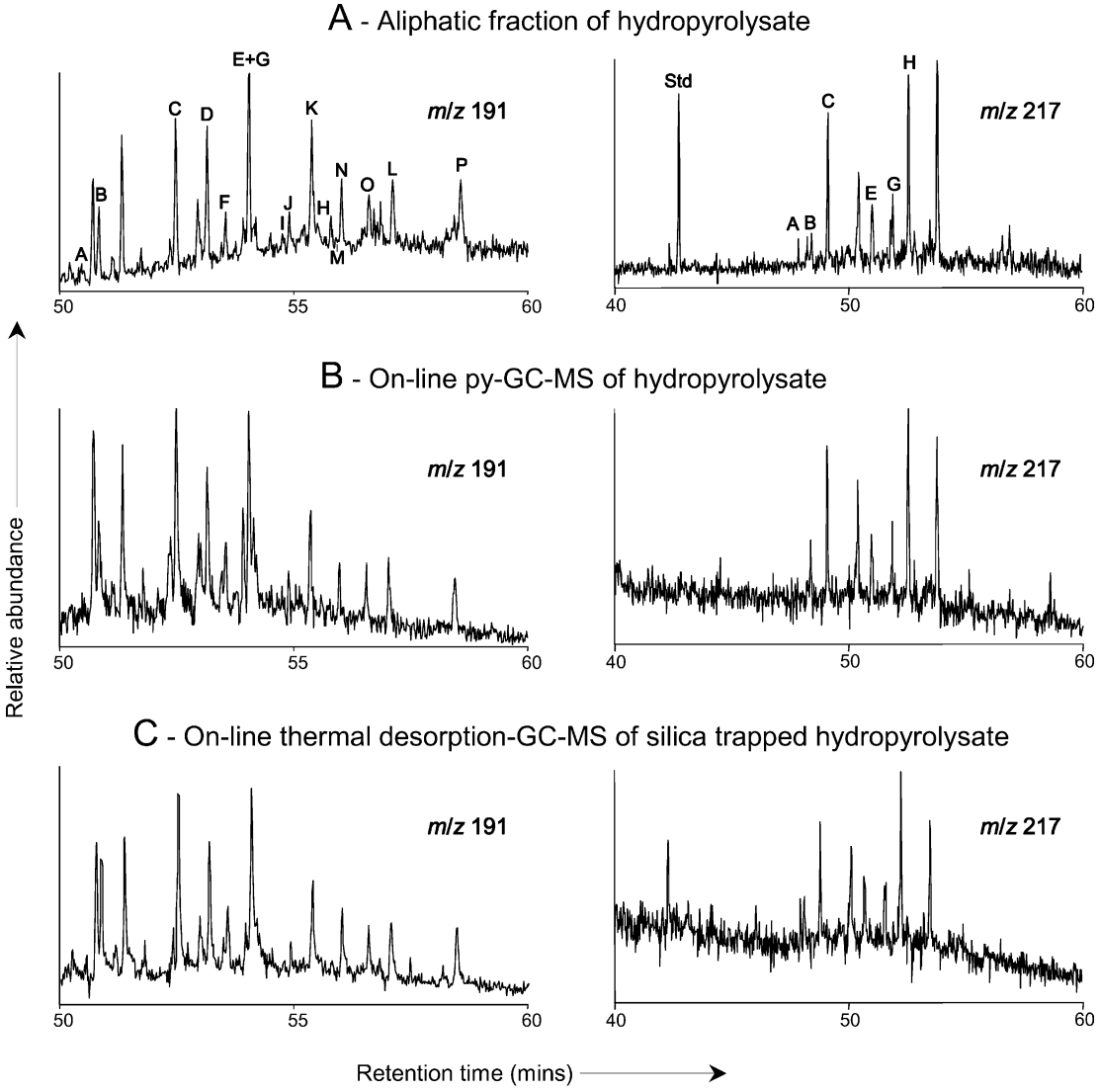

Fig. 9. Partial mass chromatograms showing distributions of selected biomarkers (*m*/*z* 191 for hopanes; *m*/*z* 217 for steranes) from the aliphatic hydrocarbon fraction of the Göynük oil shale hydropyrolysate (A), compared to the on-line py-GC–MS of the Göynük oil shale hydropyrolysate (B), and the on-line thermal desorption-GC–MS of the silica trapped Göynük oil shale hydropyrolysate (C). For peak assignments see Table 7.

silica-trapped hydropyrolysate produced very similar profiles (Figs. 8C and 9C) for both the *n*-alkanes and biomarkers to that from the py-GC-MS of the neat hydropyrolysate (Figs. 8B and 9B). Therefore, it appears that the thermal desorption of the hydropyrolysate from the trapping silica does not result in a higher degree of cracking or structural rearrangement of its components than that encountered for the neat sample. Thus, with scope for further optimisation of the pyrolysis conditions, the on-line thermal desorption of silica-trapped hydropyrolysates shows considerable potential for the fingerprinting of petroleum source rocks and coals, without encountering the loss of structural integrity commonly associated with py-GC–MS procedures.

4. Conclusions

The trapping of hydropyrolysates on silica gives results comparable to those from the conventional method using a coiled steel trap, but with a significant time saving. Both techniques result in a recovery $>80\%$ for the majority of *n*-alkanes $>n\text{-}C_{10}$ desorbed from a light crude oil under hydropyrolysis conditions, with biomarker profiles generated from a type I kerogen and crude oil asphaltenes similar for both designs of trap. Furthermore, this method of trapping has facilitated the thermal desorption-GC–MS of the silica-trapped hydropyrolysates, as demonstrated for a type I kerogen both on and off-line. This generated *n*-alkane and biomarker profiles in which secondary cracking was not significant, and which were similar to those obtained from the direct analysis of the aliphatic fraction of the hydropyrolysis products. Although further refinement of the off-line desorption heating programme in terms of both rate and final temperature is necessary to maximise the yield of aromatic and polar material, at 500 °C the yield of GC amenable aliphatic components approached 100%, in terms of both the total mass and the concentrations of individual biomarkers. Therefore, these findings demonstrate the potential of interfacing the hydropyrolysis apparatus with a GC–MS system for the rapid fingerprinting of macromolecular organic matter as a viable alternative to traditional py-GC–MS procedures.

Acknowledgements

The authors thank the Natural Environment Research Council (Ocean Margins LINK grant Nos. NER/T/S/2000/01366 and 2001/01153) for financial support and Dr Cole Robison of ChevronTexaco for providing the sample of Soldado crude oil.

References

Behar, F., Pelet, R., 1984. Characterisation of asphaltenes by pyrolysis and chromatography. Journal of Analytical and Applied Pyrolysis 7, 121–136.

Behar, F., Pelet, R., 1985. Pyrolysis-gas chromatography applied to organic geochemistry. Structural similarities between kerogens and asphaltenes from related extracts and oils. Journal of Analytical and Applied Pyrolysis 8, 173–187.

Behar, F., Pelet, R., Roucache, J., 1984. Geochemistry of asphaltenes. In: Schenck, P.A., de Leeuw, J.W., Lijmbach, G.W.M. (Eds.), Advances in Organic Geochemistry 1983, 1984. (Eds.), Organic Geochemistry 6. Pergamon Press, Oxford, pp. 587–595.

Bishop, A.N., Love, G.D., Snape, C.E., Farrimond, P., 1998. Release of kerogen-bound hopanoids by hydropyrolysis. Organic Geochemistry 29, 989–1001.

Cassani, F., Eglinton, G., 1986. Organic geochemistry of Venezuelan extra heavy oils, 1. Pyrolysis of asphaltenes: a technique for the correlation and maturity evaluation of crude oils. Chemical Geology 56, 167–183.

Connan, J., 1993. Origin of severely biodegraded oils: a new approach using biomarker pattern of asphaltene pyrolysates. In: Bordenave, M.L. (Ed.), Applied Petroleum Geochemistry. Editons Technip, Paris, pp. 456–463.

Curiale, J.A., Harrison, W.E., Smith, G., 1983. Sterane distributions of solid bitumen pyrolysates. Changes with biodegradation of crude oils in the Ouachita, Oklahoma. Geochimica et Cosmochimica Acta 47, 517–523.

Derenne, S., Largeau, C., Casadevall, E., Tegelaar, E., de Leeuw, J.W., 1988. Relationships between algal coals and resistant cell wall biopolymers of extant algae as revealed by py-GC–MS. Fuel Processing Technology 20, 93–101.

Eglinton, T.I., Larter, S.R., Boon, J.J., 1991. Characterisation of kerogens, coals and asphaltenes by quantitative pyrolysis-mass spectrometry. Journal of Analytical and Applied Pyrolysis 20, 25–45.

Gallegos, E.J., 1975. Terpane and sterane release from kerogen by pyrolysis gas chromatography mass spectrometry. Analytical Chemistry 47, 1524–1528.

Jones, D.M., Douglas, A.G., Connan, J., 1987. Hydrocarbon distributions in crude oil asphaltene pyrolysates. 1. Aliphatic compounds. Energy and Fuels 1, 468–476.

Jones, D.M., Douglas, A.G., Connan, J., 1988. Hydrous pyrolysis of asphaltenes and polar fractions of biodegraded oils. In: Mattavelli, L., Novelli, L. (Eds.), Advances in Organic Geochemistry 1987. Pergamon Press, Oxford. Organic Geochemistry 13, 981–993.

Kissin, Y.V., 1987. Catagenesis and composition of petroleum: origin of *n*-alkanes and isoalkanes in petroleum crudes. Geochimica et Cosmochimica Acta 51, 2445–2457.

Lafferty, C.J., Mitchell, S.C., Garcia, R., Snape, C.E., 1993. Investigation of organic sulphur forms in coals by high temperature-programmed reduction. Fuel 72, 367–371.

Larter, S.R., Solli, H., Douglas, A., de Lange, F., de Leeuw, J.W., 1979. Occurrence and significance of prist-1-ene in kerogen pyrolysates. Nature 279, 405–408.

Larter, S.R., Horsfield, B., 1993. Determination of structural components of kerogen by the use of analytical pyrolysis methods. In: Engel, M.H., Macko, S.A. (Eds.), Organic Geochemistry. Plenum Press, New York, pp. 271–287.

Love, G.D., Snape, C.E., Carr, A.D., Houghton, R.C., 1995. Release of covalently-bound alkane biomarkers in high yields from kerogen via catalytic hydropyrolysis. Organic Geochemistry 23, 981–986.

Love, G.D., Snape, C.E., Carr, A.D., Houghton, R.C., 1996. Changes in molecular biomarker and bulk carbon skeletal parameters of vitrinite concentrates as a function of rank. Energy and Fuels 10, 149–157.

Love, G.D., McAulay, A., Snape, C.E., Bishop, A.N., 1997. Effect of process variables in catalytic hydropyrolysis on the release of covalently-bound aliphatic hydrocarbons from sedimentary organic matter. Energy and Fuels 11, 522–531.

Love, G.D., Snape, C.E., Fallick, A.E., 1998. Differences in the mode of incorporation of biogenic sources for a type I oil shale as revealed by compound- specific stable carbon isotope ($\delta^{13}C$) measurements of aliphatic hydrocarbons released by hydrogenation and hydropyrolysis. Organic Geochemistry 28, 797–811.

Mackenzie, A.S., 1984. Applications of biological markers in petroleum geochemistry. In: Brooks, J., Welte, D. (Eds.), Advances in Petroleum Geochemistry. Academic Press, London, pp. 115–214.

Maroto-Valer, M., Love, G.D., Snape, C.E., 1997. Close correspondence between carbon skeletal parameters of kerogens and their hydropyrolysis oils. Energy and Fuels 11, 539–545.

Michaelis, W., Richnow, H.H., Jensich, A., Schulze, T., Mycke, B., 1989. Structural inferences from geochemical coal studies. In: Ittekkot, V., Kempe, S., Michaelis, W., Spitzy, A. (Eds.), Facets of modern biogeochemistry. Springer Verlag, Heidelberg, pp. 389–402.

Murray, I.P., Love, G.D., Snape, C.E., Bailey, N.J.L., 1998. Comparison of covalently-bound aliphatic biomarkers released via hydropyrolysis with their solvent-extractable counterparts for a suite of Kimmeridge clays. Organic Geochemistry 29, 1487–1505.

Murray, I.P., Snape, C.E., Love, G.D., Bailey, N.J.L., 1999. Hydropyrolysis of heavy oils for source correlation studies. Abstracts of the 19th International Meeting on Organic Geochemistry. Istanbul, 6–10 September 1999, Part 1, No. PB10, pp. 341–342.

Mykce, B., Michaelis, W., 1986. Molecular fossils from chemical degradation of macromolecular organic matter. In: Leythaeuser, D., Rullkötter, J. (Eds.), Advances in Organic Geochemistry 1985, 1986. (Eds.), Organic Geochemistry 10. Pergamon Press, Oxford, pp. 847–858.

Park, S., Jo, M.C., Park, J.B., 2000. Adsorption and thermal desorption behaviour of asphalt-like functionalities on silica. Adsorption Science and Technology 18, 675–684.

Philip, R.P., Gilbert, T.D., 1985. Source rock and asphaltene biomarker characterisation by pyrolysis-gas chromatography–mass spectrometry-multiple ion detection. Geochimica et Cosmochimica Acta 49, 1421–1432.

Philippi, G.T., 1965. On the depth, time and mechanism of petroleum generation. Geochimica et Cosmochimica Acta 29, 1021–1049.

Roberts, M.J., Snape, C.E., Mitchell, S.C., 1995. Hydropyrolysis: fundamentals. Two-stage processing and PDU operation. In: Snape, C.E. (Ed.), Geochemistry, Characterisation and Conversion of Oil Shales. NATO ASI Series C, Vol. C455, Kluwer, Dordrecht, pp. 277–295.

Robinson, N., Eglinton, G., Lafferty, C.J., Snape, C.E., 1991. Comparison of alkanes released from a bituminous coal via hydropyrolysis and low temperature hydrogenation. Fuel 70, 249–251.

Rubinstein, I., Spyckerelle, C., Strausz, O.P., 1979. Pyrolysis of asphaltenes: a source of geochemical information. Geochimica et Cosmochimica Acta 43, 111–126.

Seifert, W.K., 1978. Steranes and terpanes in kerogen pyrolysis for correlations of oils and source rocks. Geochimica et Cosmochimica Acta 42, 473–484.

Snape, C.E., Bolton, C., Dosch, R.G., Stephens, H.P., 1989. High liquid yields from bituminous coals via hydropyrolysis with dispersed catalyst. Energy and Fuels 3, 421–425.

Snape, C.E., Lafferty, C.J., Eglinton, G., Robinson, N., Collier, R., 1994. The potential for hydropyrolysis as a route for coal liquefaction. International Journal of Energy Research 18, 233–242.

van Graas, G., 1986. Biomarker distributions in asphaltenes and kerogens analysed by flash pyrolysis gas chromatography-mass spectrometry. In: Leythaeuser, D., Rullkötter, J. (Eds.), Advances in Organic Geochemistry 1985, 1986. (Eds.), Organic Geochemistry 10. Permagon Press, Oxford, pp. 1127–1135.

van Lieshout, M.P.M., Janssen, H-G., Cramers, C.A., van den Bos, G.A., 1997. Programmed-temperature vaporiser injector as a new analytical tool for combined thermal desorption-pyrolysis of solid samples application to geochemical analysis. Journal of Chromatography A764, 73–84.

van Lieshout, M.H.P.M., Janssen, H.G., Cramers, C.A., Hetem, M.J.J., Schalk, H.J.P., 1996. Characterization of polymers by multi-step thermal desorption programmed pyrolysis gas chromatography using a high temperature PTV injector. Journal of High Resolution Chromatography 19, 193–199.